Phase behaviour of polarizable colloidal hard rods in an external electric field : Supplementary Information

Thomas Troppenz[1], Laura Filion[2], René van Roij[1], Marjolein Dijkstra[2]
[1]*Institute for Theoretical Physics, Utrecht University,*
Leuvenlaan 4, 3584 CE Utrecht, the Netherlands and
[2]*Debye Institute for Nanomaterials Science, Utrecht University,*
Princetonplein 5, 3584 CC Utrecht, the Netherlands.

I. EWALD SUMS

We treated the long-range nature of the Coulomb potential using Ewald sums. We checked our implementation by reproducing the Madelung constants of NaCl for different densities. A careful investigation of the convergence properties of the Ewald sums lead us to introduce different cutoffs for the reciprocal-space Ewald vectors parallel and perpendicular to the field direction. We used $\mathbf{k}_{max} = (7\pi/L_x, 7\pi/L_y, 20\pi/L_z)$, where the last entry points in the direction of the external electric field.

II. LOW TEMPERATURE CRYSTAL STRUCTURE

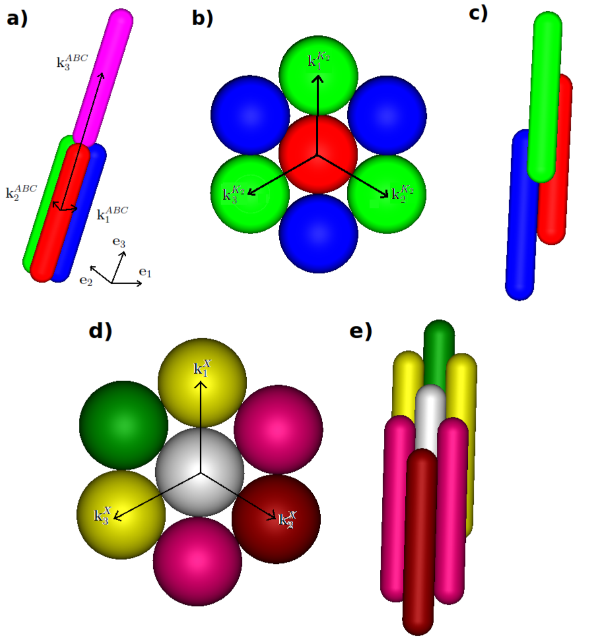

FIGURE S1. Schematic representation of the unit cells of the *ABC*, K_2 and X crystal structures. a) Unit vectors of the *ABC* crystal. b) Unit vectors of the K_2 crystal. c) Side view of the different relative height levels in the direction of the electric field in the K_2 crystal. d) Unit vectors of the X crystal. e) Side view of the different relative height levels in the direction of the electric field in the X crystal.

For $L/D = 2$, the preferred low temperature crystal structures of a system of hard polarizable spherocylinders in the double-charge model with $\delta_z = 0$ was argued to be the K_2 crystal [1]. It can be thought of as a screw-like pattern of couples of three neighboring columns each, see Fig. S1c. It is build up by the unit vectors

$$\begin{aligned} \mathbf{k}_1^{K_2} &= (D, 0, (L+D)/3), \\ \mathbf{k}_2^{K_2} &= (-D/2, \sqrt{3}D/2, (L+D)/3), \\ \mathbf{k}_3^{K_2} &= (-D/2, -\sqrt{3}D/2, (L+D)/3). \end{aligned} \tag{1}$$

We ran an NPT simulation of $L/D = 2$ rods and found that the K_2 crystal did not melt within the double-charge model with $\delta_z/D = 0.276$. However, simulating this crystal for $L/D = 5$ resulted in melting.

Therefore, we needed to find out what kind of crystal will replace it for $L/D = 5$. Our ansatz was to generalize the K_2 structure to systems of arbitrary length-to-diameter ratio L/D. Fig. S2 displays two candidate structures for the low temperature crystal (X) of as yet arbitrary L/D that reduce correctly to the K_2 structure for spherocylinders with $L/D = 2$. Here, the K_2 structure is obtained by setting $n = -k = D = (L+D)/3$ in either one of the two candidate structures. Obvious guesses for the values of k and n are given by the diameter of the rods D, $(L+D)/3$, and $D - 2\delta_z$. The last guess mentioned denotes the closest possible separation between opposite charges in two rods standing head-to-toe and is equivalent to the separation between the two charges inside the same rod $L + 2\delta_z$.

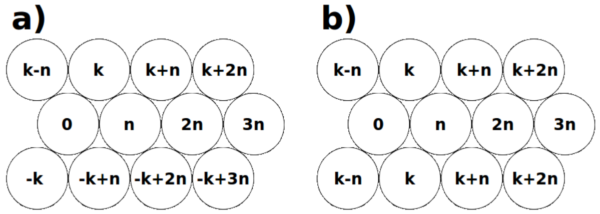

FIGURE S2. Depiction of the candidate structures for the low temperature crystal. a) Candidate structure 1 with unknown periodicity in both directions. b) Candidate structure 2 with AB stacking in one direction. The numbers inside the spheres denote the altitude of the specific rod in the direction perpendicular to the plane depicted (corresponding to the direction of the external electric field).

To decide which values to use for k and n we temporarily reduced δ_z from $\delta_z = 0.276D$ to $\delta_z = 0.25D$.

This way, we were free to focus our attention on a system of $12 \times 12 \times 6$ particles with $L/D = 5$. Note that all relevant simulations were also repeated with the correct value of δ_z. We then built up crystals with periodicity of 2, 3, 4, 6 or 12 in the directions perpendicular to the field for a variety of k and n. We investigated these phases using NPT simulations to see whether these structures remained stable, melted or transformed into different crystals. This set of NPT simulations was carried out through simulation cycles that consisted of 864 displacements, 10 volume changes and 100 movements of single columns in the direction parallel to the field. The column displacements were treated as conventional displacements of all particles in a given column at the same time. The candidate structures that we found this way were later also simulated with conventional NPT simulations, so that by comparing the results of both types of simulations we were able to conclude that we implemented the column displacements correctly. We did conclude however that the displacements of whole columns significantly decreased the number of simulation cycles necessary for the equilibration of the system.

Only one of the candidate structures that we guessed remained stable during the simulation. We denote this one as candidate $2E$ ($C2E$). However, some of our guesses transformed to a modified version of $C2E$ that we denoted by $C2E^*$. Candidate structure $C2G$ transformed into something that almost looked like a crystal. We were able to deduce the structure of this crystal and denoted it by $C2W$. For a system of $12 \times 12 \times 6 = 864$ particles these three, $C2E$, $C2E^*$, and $C2W$, together with the conventional ABC crystal, are our best guesses for the structure of the low temperature crystal. $C2E$ has the lowest free energy, while the free energy of $C2E^*$ and $C2W$ is about 0.3 percent higher for a range of densities. A sketch showing the structure of the three candidates is shown in Fig. S3. Snapshots of these phases can be seen in Fig. S4.

Interestingly, if we rewrite the unit vectors of the K_2 crystal as

$$\begin{aligned}
\mathbf{k}_1^X &= (D, 0, D), \\
\mathbf{k}_2^X &= (-D/2, \sqrt{3}D/2, -2D), \\
\mathbf{k}_3^X &= (-D/2, -\sqrt{3}D/2, D),
\end{aligned} \tag{2}$$

we recover the $C2E$ crystal for $L/D = 5$. Fig. S1 displays the unit cells of the ABC, K_2 and X ($C2E$) crystal structures.

As $C2E$ had the lowest free energy of the three structures, in this paper, we performed our simulations with $C2E$. Throughout the main paper, crystal X refers to $C2E$.

---

[1] M. Rotunno, T. Bellini, Y. Lansac, M.A. Glaser, J. Chem. Phys. **121**, 5541 (2004).

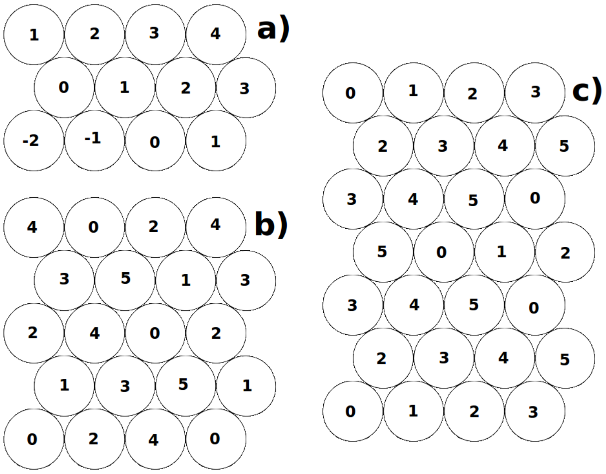

FIGURE S3. Candidate structures for the low temperature crystal. a) $C2E$, b) $C2W$, and c) $C2E^{*}$. The numbers denote the altitude in the direction parallel to the external field (in units of D=1).

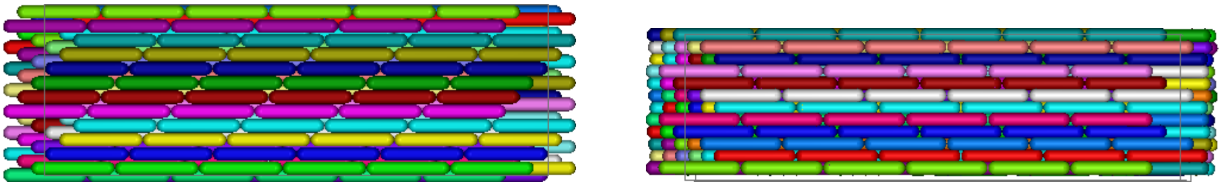

(a) $C2E$, (0,1,0)

(b) $C2E$, (0,0,1)

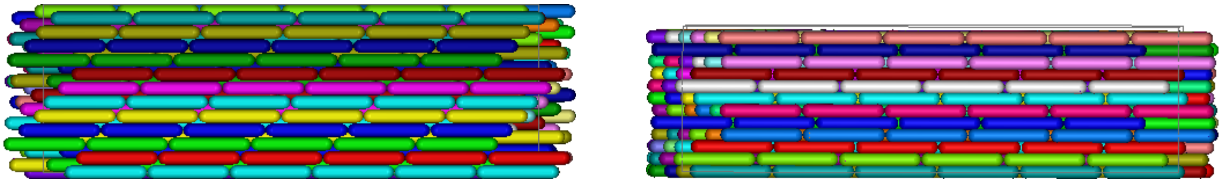

(c) $C2E^{*}$, (0,1,0)

(d) $C2E^{*}$, (0,0,1)

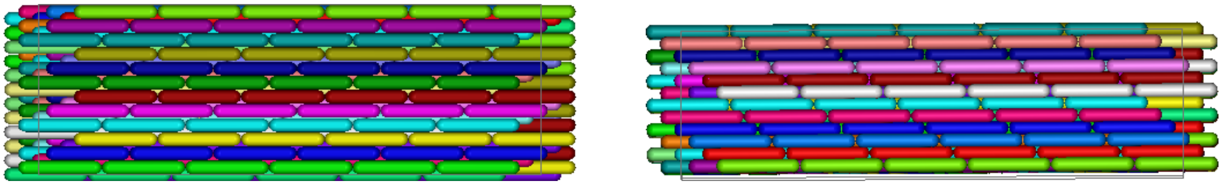

(e) $C2W$, (0,1,0)

(f) $C2W$, (0,0,1)

FIGURE S4. Snapshots of the three candidate structures. $C2E$, $C2E^{*}$, and $C2W$.